

COMPUTATION OF SCATTERING FROM ANISOTROPICALLY COATED BODIES USING CONFORMAL FDTD

H.-X. Zheng

Wireless Communications Research Centre
Department of Electronic Engineering
City University of Hong Kong
Kowloon, Hong Kong

X.-Q. Sheng

Institute of Electronics
Chinese Academy of Sciences
Beijing, P.R. China

E. K.-N. Yung

Wireless Communications Research Centre
Department of Electronic Engineering
City University of Hong Kong
Kowloon, Hong Kong

Abstract—A conformal FDTD approach is developed to compute scattering from anisotropically coated bodies. Comparisons between the standard and conformal FDTDs are numerically carried out to demonstrate the advantages of the conformal FDTD. Scattering of anisotropic dielectric sphere is computed and compared with the analytical results to further validate the developed approach. Several new results of scattering by anisotropically coated bodies are also given in the paper.

1 Introduction

2 Formulations

3 Numerical Results

4 Conclusions

References

1. INTRODUCTION

The scattering from conducting bodies can be significantly changed by putting on coating. It is one of major ways to reduce the radar cross section (RCS) of aircraft by making suitable coating. To design coating, the computation of scattering from coated bodies has been an important problem.

The coating can be dealt as approximate boundary conditions (ABCs) [1]. This treatment is essentially approximate and has various limitations. To obtain accurate RCS for general coated bodies, a rigorous method of moment (MoM) based on surface integral equation has been developed [2]. Due to the dense MoM matrix, this method is restricted to only small electric size bodies. Recently, a hybrid FEM/MLFMA has been developed for large coated bodies [3]. This method reaches the computational complexity of $O(N_i + N_s \log N_s)$. (N_i and N_s denotes the number of unknowns in the interior and exterior region respectively.) The difficulty of this method is that it experiences a slow convergence for bodies with thick coating.

The goal of this work is to develop a time-domain accurate and efficient approach to compute scattering from conducting bodies with anisotropic coating using conformal FDTD [4, 5]. In this study, we first compute the scattering by a conducting cube to demonstrate the accuracy and efficiency of the standard FDTD and second-order Mur absorbing boundary condition (ABC) [6]. Then scattering of conducting sphere and coated sphere are computed by the standard and conformal FDTDs to demonstrate the advantages of the conformal FDTD. Next, Scattering of anisotropic dielectric sphere is computed and compared with the analytical results to further validate the developed approach. Several new results of scattering by anisotropically coated bodies are also given at last.

2. FORMULATIONS

It is well known that the electromagnetic field in the anisotropic material is governed by the following Maxwell's equations

$$\nabla \times \mathbf{E} = -\mu_0[\mu_r] \frac{\partial \mathbf{H}}{\partial t} - [\sigma_m] \mathbf{H} \quad (1)$$

$$\nabla \times \mathbf{H} = \epsilon_0[\epsilon_r] \frac{\partial \mathbf{E}}{\partial t} + [\sigma_e] \mathbf{E} \quad (2)$$

where we only consider the case of the diagonal form of $[\epsilon_r]$, $[\mu_r]$, $[\sigma_e]$, and $[\sigma_m]$ in this paper, namely, we have

$$[a] = \begin{bmatrix} a_x & 0 & 0 \\ 0 & a_y & 0 \\ 0 & 0 & a_z \end{bmatrix}, \quad a = \epsilon_r, \mu_r, \sigma_e, \sigma_m \quad (3)$$

To discretize (1) and (2), we arrange the locations of the components of the electromagnetic field in the Yee's cell as those for isotropic material [7]. Since the procedure for deriving the updating formulae of all six components is similar, we here only consider the z components E_z and H_z . Expanding (1) and (2), we can obtain

$$\frac{\partial H_y}{\partial x} - \frac{\partial H_x}{\partial y} = \epsilon_0 \epsilon_z \frac{\partial E_z}{\partial t} + \sigma_{ez} E_z \quad (4)$$

$$\frac{\partial E_y}{\partial x} - \frac{\partial E_x}{\partial y} = -\mu_0 \mu_z \frac{\partial H_z}{\partial t} - \sigma_{mz} H_z \quad (5)$$

Similar to the case of isotropic material, (4) and (5) can be easily discretized as

$$E_z \Big|_{i,j,k+1/2}^{n+1} = c_1 E_z \Big|_{i,j,k+1/2}^n + c_2 \left[\left(H_y \Big|_{i+1/2,j,k+1/2}^{n+1/2} - H_y \Big|_{i-1/2,j,k+1/2}^{n+1/2} \right) / \Delta x \right. \\ \left. - \left(H_x \Big|_{i,j+1/2,k+1/2}^{n+1/2} - H_x \Big|_{i,j-1/2,k+1/2}^{n+1/2} \right) / \Delta y \right] \quad (6)$$

$$H_z \Big|_{i+1/2,j+1/2,k}^{n+1/2} = d_1 H_z \Big|_{i+1/2,j+1/2,k}^{n-1/2} + d_2 \left[\left(E_y \Big|_{i+1,j+1/2,k}^n - E_y \Big|_{i,j+1/2,k}^n \right) / \Delta x \right. \\ \left. - \left(E_x \Big|_{i+1/2,j+1,k}^n - E_x \Big|_{i+1/2,j,k}^n \right) / \Delta y \right] \quad (7)$$

with

$$c_1 = \frac{2\epsilon_0 \epsilon_z \Big|_{i,j,k+1/2} - \Delta t \sigma_z \Big|_{i,j,k+1/2}}{2\epsilon_0 \epsilon_z \Big|_{i,j,k+1/2} + \Delta t \sigma_z \Big|_{i,j,k+1/2}} \quad (8)$$

$$c_2 = \frac{2\Delta t}{2\epsilon_0 \epsilon_z \Big|_{i,j,k+1/2} + \Delta t \sigma_z \Big|_{i,j,k+1/2}} \quad (9)$$

$$d_1 = \frac{2\mu_0 \mu_z \Big|_{i+1/2,j+1/2,k} - \Delta t \sigma_z \Big|_{i+1/2,j+1/2,k}}{2\mu_0 \mu_z \Big|_{i+1/2,j+1/2,k} + \Delta t \sigma_z \Big|_{i+1/2,j+1/2,k}} \quad (10)$$

$$d_2 = \frac{-2\Delta t}{2\mu_0 \mu_z \Big|_{i+1/2,j+1/2,k} + \Delta t \sigma_z \Big|_{i+1/2,j+1/2,k}} \quad (11)$$

where the meaning of superscript and subscript in (6)–(11) is the same as that in [7]. The equations (6) and (7) are the standard updating formulae of E_z and H_z for anisotropic material. Although this standard FDTD scheme can be employed to model curved surface by using staircase approximation, it is not accurate and efficient. To be more accurate, we need to employ the conformal FDTD scheme. For coated bodies, we will meet two kinds of curved surface: curved conducting surface and curved interface between different materials. For curved conducting surface, we apply Faraday's law to derive the updating formulae [4]. The derived formulae for E-field are the same as those in the standard FDTD scheme, but those for H-field are changed. For example, (7) is changed as

$$H_z \Big|_{i+1/2, j+1/2, k}^{n+1/2} = d_1 H_z \Big|_{i+1/2, j+1/2, k}^{n-1/2} + d'_2 \left[\left(E_y \Big|_{i+1, j+1/2, k}^n l_y \Big|_{i+1, j+1/2, k} - E_y \Big|_{i, j+1/2, k}^n l_y \Big|_{i, j+1/2, k} \right) - \left(E_x \Big|_{i+1/2, j+1, k}^n l_x \Big|_{i+1/2, j+1, k} - E_x \Big|_{i+1/2, j, k}^n l_x \Big|_{i+1/2, j, k} \right) \right] \quad (12)$$

with

$$d'_2 = \frac{-2\Delta t}{\left(2\mu_0\mu_z \Big|_{i+1/2, j+1/2, k} + \Delta t\sigma_z \Big|_{i+1/2, j+1/2, k} \right) A_z} \quad (13)$$

where A_z is the face area of the cell excluding the metallic region, and l_x and l_y are the cell length along the x - and y -directions, respectively, outside the metal. For the curved interface between different material, we here employ a newly-developed technique [5], which is very suitable to be extended to anisotropic case. The key point of this technique is to define effective material parameters for every component of electromagnetic field respectively. For example, as shown in Fig. 1, we can define the effective dielectric constants, $\epsilon_y^e|_{i, j+1/2, k}$, $\epsilon_z^e|_{i, j, k+1/2}$, for $E_y|_{i, j+1/2, k}$, $E_z|_{i, j, k+1/2}$ respectively as

$$\epsilon_y^e \Big|_{i, j+1/2, k} = [\Delta y_2 \epsilon_{y2} + (\Delta y - \Delta y_2) \epsilon_{y1}] / \Delta y \quad (14)$$

$$\epsilon_z^e \Big|_{i, j, k+1/2} = [\Delta z_2 \epsilon_{z2} + (\Delta z - \Delta z_2) \epsilon_{z1}] / \Delta z \quad (15)$$

Note that the dielectric constants for $E_y|_{i, j+1/2, k+1}$, $E_z|_{i, j+1, k+1/2}$ in the same cell need not to do average since the edges where these fields locate are uniform.

After the updating formulae for anisotropically coated bodies are derived, the FDTD algorithm can be obtained as usual. In this paper,

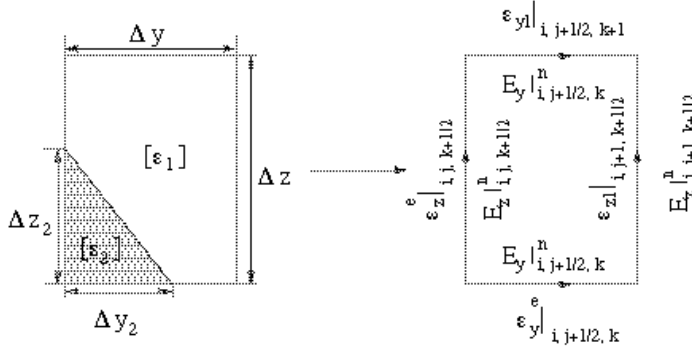


Figure 1. Linear averaging procedure for curve dielectric interface in the conformal FDTD scheme.

the second-order Mur ABC is used. The Gaussian pulse incident plane wave is incorporated into the total-field/scattering-field formulation as did in [7]. The far field is computed concurrently with the normal FDTD time-stepping with a technique developed in [8].

3. NUMERICAL RESULTS

In this section we will show numerical results to validate the above described conformal FDTD scheme. The first example is the scattering from a conducting cube, whose side length $a = 0.5$ m. Before showing numerical results, we would like to point out the parameters in the calculation in this paper. We take the cell size $\Delta x = \Delta y = \Delta z = \Delta = 0.01$ m and $\Delta t = 0.5\Delta/c$ (c is the speed of light in the free space). The incident plane wave is Gaussian pulse, written as

$$E(t) = \exp(-4\pi(t - t_0)^2/\tau^2) \quad (16)$$

where t_0 is chosen as $80\Delta t$ and $\tau = 3t_0$. The second-order Mur ABC is placed at an enclosed surface 0.1 m away from the bodies. Figure 2 presents the comparison of the backscatter RCS between the measured data [10] and our calculated results, demonstrating the accuracy of the FDTD scheme. The second example is the scattering from the conducting sphere, whose diameter $d = 1$ m. Figure 3 presents the comparison of the backscatter RCS between analytical Mie series, the standard FDTD and the conformal FDTD, from which we see that the conformal FDTD has a big improvement in accuracy over the standard FDTD at the high frequencies. The third example is a

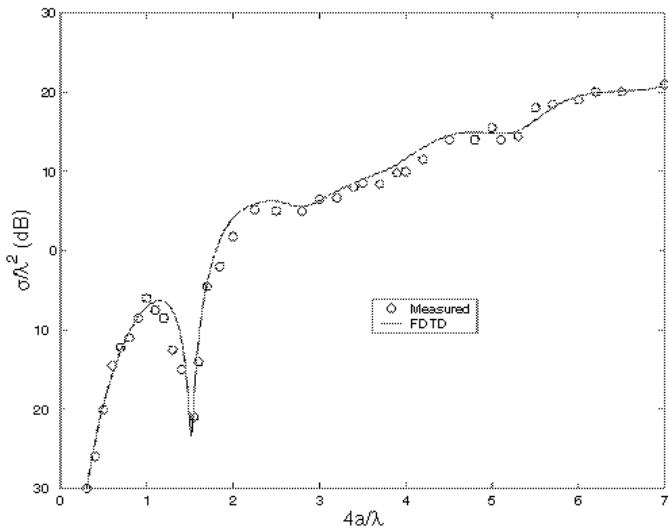


Figure 2. Backscatter RCS from a conducting cube.

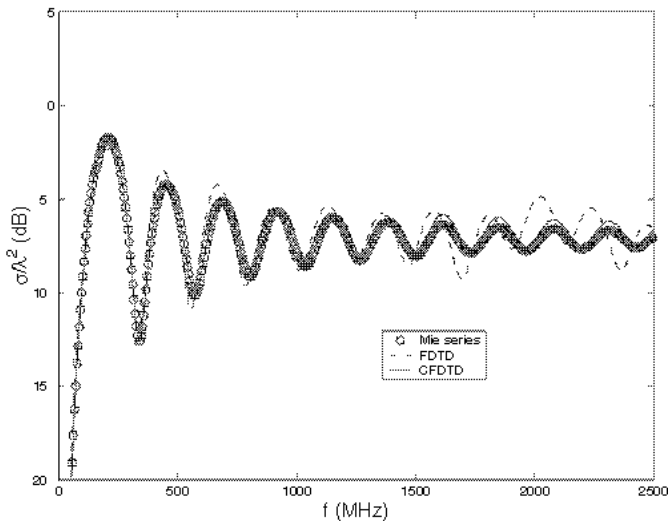


Figure 3. Backscatter RCS from a conducting sphere.

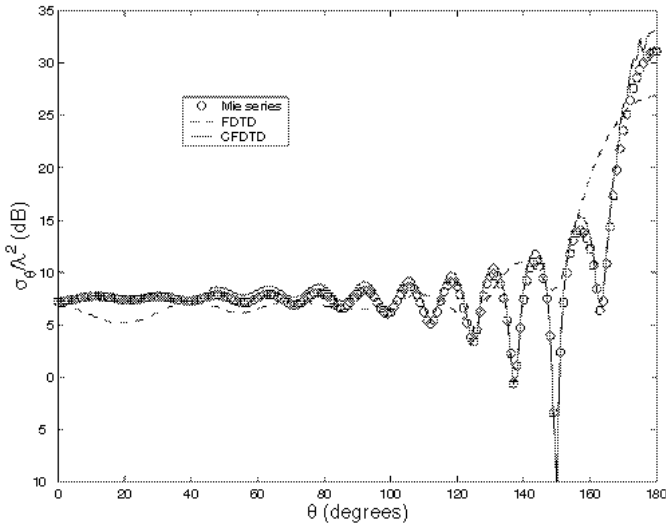


Figure 4. Bistatic RCS from a coated sphere.

coated sphere, whose diameter of conducting sphere is still $d = 1$ m and thickness of coating $s = 0.08$ m and relative dielectric constant $\epsilon_r = 5.6$. Its bistatic RCS at $f = 1.5$ GHz is shown in Fig. 4. Again, it can be seen that the conformal FDTD is much more accurate than the standard FDTD. The fourth example is the anisotropic dielectric sphere made up of titanium dioxide (TiO_2), whose diameter $d = (1/2\pi)\lambda_0$, and $\epsilon_{rx} = \epsilon_{ry} = 7.179$, $\epsilon_{rz} = 0.913$. Figures 5–7 present the scattering pattern at the different incident directions and polarizations: $\mathbf{E}_{inc} = \mathbf{e}_x E_t \exp(ikz)$, $\mathbf{E}_{inc} = \mathbf{e}_y E_t \exp(ikx)$, $\mathbf{E}_{inc} = \mathbf{e}_z E_t \exp(ikx)$, respectively. It can be seen that our calculated results have good agreement with those from the coupled dipole approximation method [9], demonstrating validity of our conformal FDTD for anisotropic case. Note that the cross-polarization component under x incident direction is observed in Figs. 6–7 due to anisotropic material, whereas this cross-polarization component is very small under z incident direction and cannot be observed in Fig. 5. Finally, we calculate the scattering by a anisotropically coated sphere and cube. Figure 8 presents the bistatic RCS from the anisotropically coated sphere, whose diameter $d = 1$ m, thickness $s = 0.08$ m, and relative dielectric constant $\epsilon_x = \epsilon_y = 5.6$, $\epsilon_z = 0.92$ at frequency $f = 1.5$ GHz. Figure 9 presents the backscatter RCS from the anisotropically coated cube, whose side length $a = 0.45$ m, thickness of coating $s = 0.025$ m, the relative dielectric constant $\epsilon_{rx} = \epsilon_{ry} = 5.6 - j2.28$, $\epsilon_{rz} = 7.0 - j1.0$.

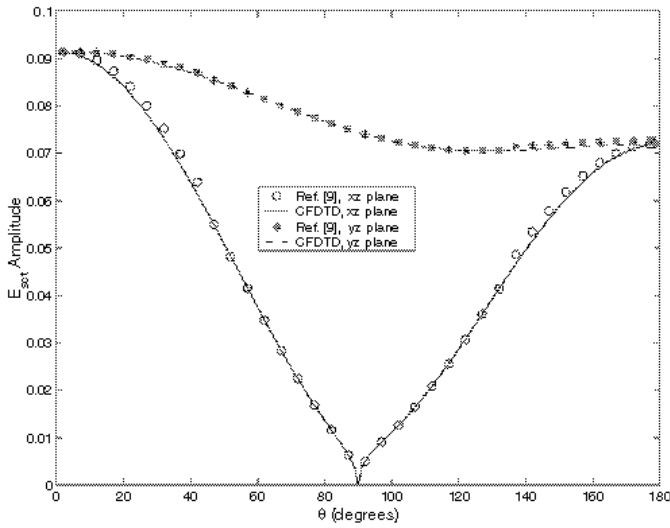


Figure 5. Scattering patterns from an anisotropic sphere under $\mathbf{E}_{\text{inc}} = \mathbf{e}_x E_t \exp(ikz)$.

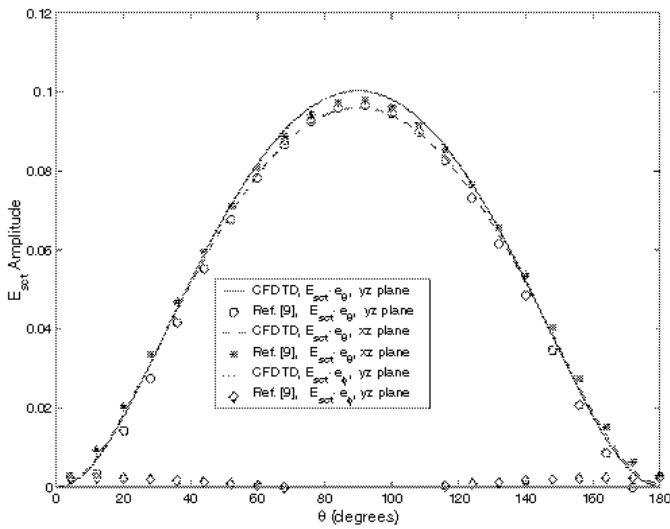


Figure 6. Scattering patterns from an anisotropic sphere under $\mathbf{E}_{\text{inc}} = \mathbf{e}_z E_t \exp(ikx)$.

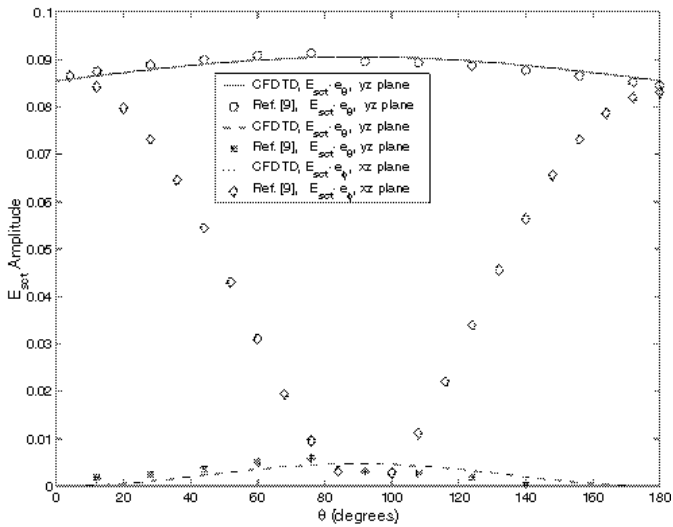


Figure 7. Scattering patterns from an anisotropic sphere under $\mathbf{E}_{inc} = \mathbf{e}_y E_t \exp(ikx)$.

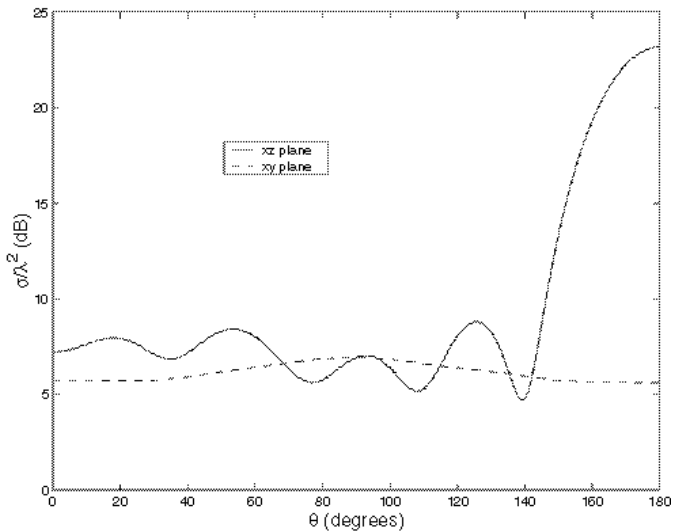


Figure 8. Bistatic RCS from an anisotropically coated sphere.

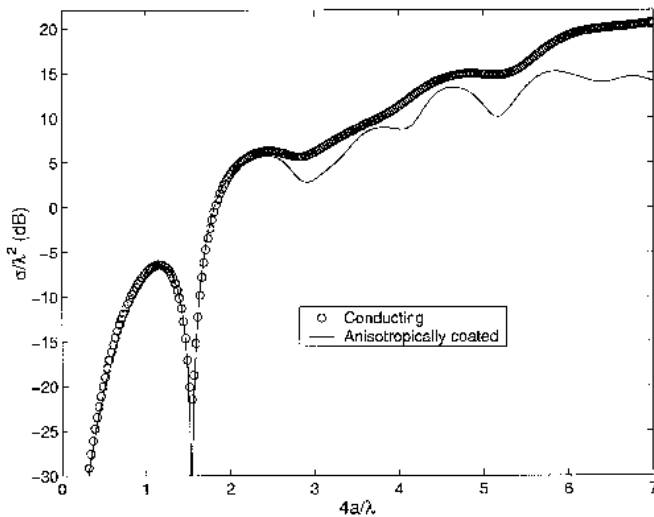


Figure 9. Backscatter RCS from an anisotropically coated cube.

4. CONCLUSIONS

A conformal FDTD approach is developed to compute scattering from anisotropically coated bodies. Numerical results demonstrate that the conformal FDTD has a big improvement in accuracy over the standard FDTD. The computation of scattering of anisotropic dielectric sphere validate the developed approach. Several new numerical results of scattering from anisotropically coated bodies are also given in the paper.

REFERENCES

1. Senior, T. B. A., "Approximate boundary conditions," *IEEE Trans. Antennas Propag.*, Vol. 29, No. 5, 826–829, Sept. 1981.
2. Rao, S. M., C. C. Cha, R. L. Cravey, and D. L. Wilkes, "Electromagnetic scattering from arbitrary shaped conducting bodies coated with lossy materials of arbitrary thickness," *IEEE Trans. Antennas Propag.*, Vol. 39, No. 5, 627–631, May 1991.
3. Sheng, X. Q., J. M. Jin, J. M. Song, C. C. Lu, and W. C. Chew, "On the formulation of hybrid finite-element and boundary-integral method for 3D scattering," *IEEE Trans. Antennas Propag.*, Vol. AP-46, 303–311, Mar. 1998.

4. Jurgens, T. G., A. Taflove, K. R. Umashankar, and T. G. Moore, "Finite difference time-domain modeling of curved surfaces," *IEEE Trans. Antennas Propag.*, Vol. AP-40, 357-366, 1992.
5. Yu, W. and R. Mittra, "A conformal finite difference time domain technique for modeling curved dielectric surfaces," *IEEE Microwave and Wireless Components Letters*, Vol. 11, No. 1, 25-27, Jan. 2001.
6. Kunz, K. S. and R. J. Luebbers, *The Finite Difference Time Domain Method for Electromagnetics*, CRC Press, Boca Raton, FL, 1993.
7. Taflove, A. and S. C. Hagness, *Computational Electrodynamics: The Finite Difference Time Domain Method*, 2nd Edition, Artech House, Norwood, MA, 2000.
8. Luebbers, R. J., K. S. Kunz, M. Schneider, and F. Hunsberger, "A finite-difference time-domain near zone to far zone transformation," *IEEE Trans. Antennas Propag.*, Vol. 39, 429-433, Apr. 1991.
9. Varadan, V. V., A. Lakhtakia, and V. K. Varadan, "Scattering by three-dimensional anisotropic scatterers," *IEEE Trans. Antennas Propag.*, Vol. 37, 800-802, June 1989.
10. Yaghjian, A. D. and R. V. McGahan, "Broadside radar cross-section of a perfectly conducting cube," *IEEE Trans. Antennas Propag.*, Vol. 33, 321-329, Mar. 1985.